Romanian Reports in Physics **69**, 502 (2017)

IMPACT OF FUNCTIONALISATION ON THE TRANSPORT THROUGH THE ADENINE MOLECULE

KHADIJEH KHALILI[1,a], HOSSAIN MILANI MOGHADDAM[1,b]

[1]Department of Solid State Physics, University of Mazandaran, Babolsar, 47416-95447, Iran
[a]*Email*: *kh.khalili@stu.umz.ac.ir*
[b]Corresponding author *Email*: *milani@umz.ac.ir*

Received May 31, 2016

Abstract. The influence of electron donating and accepting functional groups OCH_3, CH_3/CN and CHO on electron transport properties of a single Adenine-based molecular junction has been numerically studied using the density functional based tight-binding method. It has been found that the above mentioned electron acceptor groups have a strong effect on transmission of the molecular junction resulting in a strong drop of conductance. On the other hand, in both electron donating and accepting categories, the partial density of states indicates that the delocalized nature of the p-orbitals of the adenine is responsible for the impressive effect of the functional group with π-symmetric valence orbitals. Furthermore, the CN functional group has an effect on the current-voltage characteristics of the junction, which is distinct from the effects of all the other functional groups studied here.

Key words: Functional group; Single molecule; Adenine; Density functional theory.

1. INTRODUCTION

Single molecular junctions are of interest both for improving our fundamental understanding of electronic transport at the nanoscale and for the development of novel electronic devices. The vast flexibility in design and functionality of the single molecular devices is one of the main advantages of this type of electronics. Transport properties of the molecule in a coherent transport regime depend on the intrinsic properties of the molecule, including their length and conformation, the chemical groups anchoring the molecule to the electrodes, the contact geometry of the molecule-electrode interface, and its functionalization [1–4]. In particular, there are many experimental and theoretical works on the influence of specific functional groups on single molecule junctions. For instance, in 2007, Venkataraman *et al.* have measured the conductance of diamino benzene with different substitutes (halogenes, OCH_3, CH_3, and CN) that shift the molecular levels relative to the Au Fermi level in the single molecule junctions resulting in a chemical gating of the junction conductance [5]. Complementary density functional theory (DFT) studies, by Mowbray *et al.*, on the influence of five classes of functional groups on the transport properties

of benzenedithiolate and benzenediamine molecular junctions with gold electrodes showed that the qualitative change in conductance due to a given functional group can be predicted from its known electronic effect [6]. In addition, the quantum transport through tour wires functionalized with NO_2 and NH_2 side groups was studied theoretically by Kala *et al.* and they observed a significant effect of the functionalization on the transport behavior of the molecular system [7]. In all mentioned studies, functionalization caused a shift in the position of either highest occupied molecular orbital (HOMO) or lowest unoccupied molecular orbital (LUMO) levels resulting in a low change in conductance.

The possibility to exploit DNA bases in mesoscopic electronic devices have been studied intensively both experimentally and theoretically [8–11]. Overlapping π orbitals of the DNA base pairs provide a channel for the migration of an extra charge injected into it. In the current study, the molecule of interest is adenine, one of the most abundant biochemical molecules on Earth. Surprisingly no dedicated studies are available on functionalized Adenine at the single-molecule level. With this contribution, we aim to do a first attempt to shed light on the behavior of different functional groups, as exemplified by OCH_3, CH_3, CN, and CHO, on the transport properties of this molecular junction. The main purpose of this study is not only to show the remarkable effect of substitute groups on the position of the frontier orbitals and on the conductance but also to improve our fundamental understanding of this effect. Also, the impact of functional groups on the I-V characteristics of the adenine-based single molecular junction is studied. The calculations are performed using the density functional based tight binding method (DFTB) combined with nonequilibrium Green's function formalism (NEGF) [12].

2. SIMULATION METHOD

The electronic structure of systems under investigation is obtained with the density functional based tight-binding method (DFTB) [13–15]. This approach being approximate shows still a useful accuracy and has been successfully employed for calculations of various physical properties including band structures, excitations, Raman spectra, geometries, polarizabilities, and conductances [16–21]. At the same time it reveals higher computational efficiency and better scaling with the system size as compared to the *ab initio* methods. Compared to the DFT methods with semi-local functionals the execution time of DFTB implementations is usually three orders of magnitude smaller. Due to this fact, the DFTB method is chosen for the study of Adenine molecular junctions.

2.1. SCC-DFTB FORMALISM

Self consistent charge DFTB (SCC-DFTB) [22] is derived from a Taylor series expansion of the Kohn-Sham total energy [23] around a properly chosen reference density $\rho_0(r)$ up to a second order in density fluctuation $\delta\rho(r)$. The reference density is usually chosen to be a superposition of atomic densities. The total energy then reads

$$E_{total} = E_{TB} + E_2 + E_{rep}, \tag{1}$$

where E_{TB} is the usual tight-binding band energy, that is, the occupation weighted sum of the single particle eigenvalues of the zeroth-order DFTB Hamiltonian. E_{rep} is a short-ranged repulsive interaction term and E_2 is an electrostatic interaction term which takes into account charge fluctuations. The matrix elements of the zeroth-order Hamiltonian are transformed to the molecular frame by the Slater-Koster rules [24] and a consistent set of transferable pair potentials must be created by combined DFT/DFTB calculations on reference structures. These matrix elements have to be known (as parameter set) at the start of any calculation. We use the parameter set which was developed for gold-thiolates compounds with atoms, including S, Au, N, C, and H [25].

If we consider now the case with two contacts and a central molecular (M) region, under the assumption that there is no direct interaction between contacts, we can calculate the transmission coefficient between the R contact and the L contact as

$$T_{RL} = Tr[\Gamma_R G_M^r \Gamma_L G_M^a] \tag{2}$$

where $\Gamma_{R/L} = i[\Sigma_{R/L}^r - \Sigma_{R/L}^a]$ is the coupling with the contact leads, Σ is the self-energy term, and r/a stands for retarded/advanced Green's function. G_M describes the dynamics of the electrons inside the molecular system and can be expressed as $G_M^{r/a} = [E\mathbf{S}_M - \mathbf{H}_M - \mathbf{\Sigma}^{r/a}]^{-1}$. $\mathbf{H}_M$ describes the Hamiltonian for the full system and $\mathbf{S}_M$ is the overlap matrix between orbitals [26]. In addition to calculate the conductance, nonequilibrium Green's function formalism (NEGF) was used with SCC-DFTB. The current was calculated by Landauer-Buttiker formula [27]

$$I = \frac{2e^2}{h} \int_{\mu_L}^{\mu_R} T(E, V_b)[f(E-\mu_L) - f(E-\mu_R)]\,\mathrm{d}E \tag{3}$$

where μ_R and μ_L are the chemical potentials of the right and left electrodes, e is the electron charge, h is Planck's constant, $f(E, \mu_{L/R})$ are the Fermi distributions of electrons in the left and right electrodes; $T(E, V_b)$ represents the electronic transmission probability, and V_b is the applied bias voltage across the electrodes. An applied bias V_b will shift the chemical potential of the left and right electrodes to $\mu_L = E_F - |e|V/2$ and $\mu_R = E_F + |e|V/2$ where E_F is the Fermi energy.

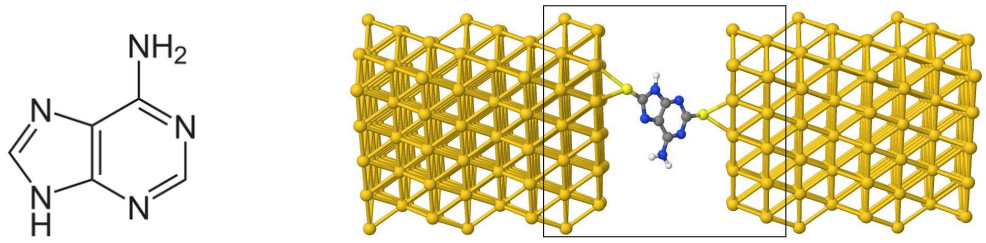

(a) (b)

Fig. 1 – (a) Schematic of the adenine molecule. (b) The corresponding model system based on Adenine for the single-molecule situation. The carbon atoms are shown in gray, the nitrogen atoms in blue, and the hydrogen atoms in white. The central extended molecule is indicated as one rectangle.

2.2. CALCULATION PROCEDURE

As a molecular junction, the adenine molecule (Fig. (1a)) connected to two gold electrodes has been investigated. The two-probe system is based on the three region partition of the device of interest: left electrode (L), right electrode (R) and central region (C). The left and the right bulk electrodes are built of six gold layers grown along the (111) direction. The central extended molecule (EM) consists of the molecule and two layers of gold that are enough long to avoid any interaction between the molecule and the next supercell in this model. The full structure is shown in Fig. (1b). The sulfur atom, as a terminal group, is chosen not only on the basis of its binding selectivity, but also its ability to provide maximum conductivity between the molecule and the metallic electrode [28]. To reach minimum energy for each configuration, before performing the calculations, all structures are optimized. The modeling of the considered systems is usually performed by optimizing the functionalized thiolated structures in gas-phase and subsequently connecting them to the gold electrodes *via* the bridge site, with the S-Au bond distance of 2.59 Å and the distance of S from the vertical Au surface equal 2.14 Å [29]. This results in a distance of 12.02 Å between the two electrodes. The surface Brillouin zone was sampled on a 4×4 k-point Monkhorst-Pack grid [30]. We use periodic boundary conditions in the direction parallel to the interface between the adenine and gold electrodes, plus a supercell approximation. Then, we applied bias voltage along the structures and computed the current. The applied bias voltage was increased from 0 to 2.5 V in steps of 0.25 V.

3. RESULTS AND DISCUSSION

At first, we calculated the zero-bias energy-dependent electron transmission for the bare adenine molecule device as depicted in Fig. (2a). We observe the Au

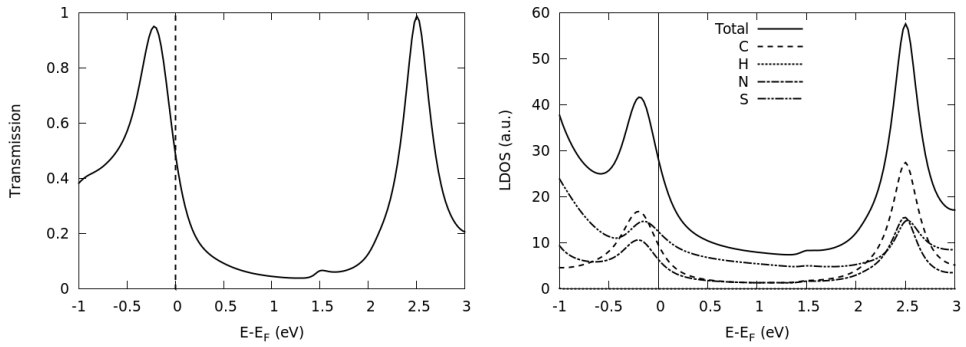

(a) (b)

Fig. 2 – (a) The energy-dependent electron transmission and (b) the local density of states (LDOS) of the bare adenine molecule device at zero-bias. Vertical lines indicate the Au Fermi level.

Fermi level (E_F) to be positioned just above the HOMO level. The relatively close proximity of the HOMO to E_F indicates that adenine should have good conducting properties which is in good agreement with the previous $ab-initio$ Green's function study [11]. The small difference between our study and the one reported in Ref. [11] could be due of the different contact geometries or different molecular conformations used. To analyze the band alignment of the molecular energy levels to the electrode Fermi level of the molecular junction Au-(S-bare adenine-S)-Au, we calculated local density of states (LDOS) that is presented in Fig. (2b). There is a main peak just below Au Fermi level that corresponds to the transmission probability peak. The HOMO state is near the Fermi level which indicates that the conduction through this structure is *via* a hole-tunneling mechanism.

Then, we investigated the effect of the functional groups on the electronic properties of the adenine molecular junction at the 3 positions. We considered the effect of different functional groups from each of the main four electronic categories [31], as shown in Table 1, on the transport properties of the molecular junction. The selection of functional groups comprises different chemical classes and are, by no means, the only possibilities. The electron donating groups (EDG) are activating groups and can be recognized by lone pairs on the atom adjacent to the p system. The electron withdrawing groups (EWG) are deactivating groups and can be recognized either by the atom adjacent to the p system having several bonds to more electronegative atoms. There is one additional functional group with not only σ-accepting but also with π-donating effects (e.g. Halogens), that was ignored in this study, because of a limitation on the used parameter set.

The central adenine molecule with different functional groups is presented in Fig. (3). The calculated conductance, $G = G_0T(E_F)$, where $G_0 = 2e^2/h$, for all

Table 1 Selected functional groups categorized by electronic effect.

Electronic effect	**Functional group**
π-donor	-OCH_3 (Methoxy)
σ-donor	-CH_3 (Methyl)
π-acceptor	-CN (Nitrile)
σ-acceptor	-CHO (Aldehyde)

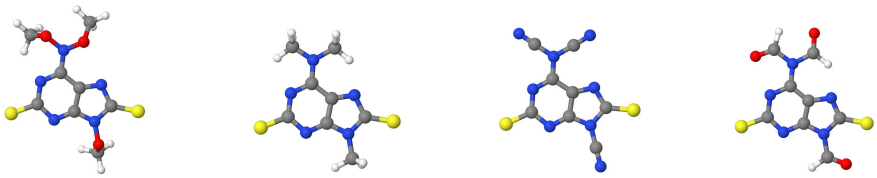

(a)OCH_3 (b)CH_3 (c)CN (d)CHO

Fig. 3 – The central adenine molecule with different functional groups.

structures is presented in Table 2. We observed that the electron donating groups increase the conductance while the electron withdrawing groups decrease it. This finding is in a good agreement with previous theoretical and experimental results [5, 6, 32]. It shows the conductance of the considered structure is strongly affected by the functionalization.

Table 2 Conductance G of the bare and functionalized adenine between gold (111) surfaces.

Functional species	$\mathbf{G[2e^2/h]}$
$H \times 3$	0.82
$OCH_3 \times 3$	0.86
$CH_3 \times 3$	0.85
$CN \times 3$	0.21
$CHO \times 3$	0.13

From the transmission probability curve in Fig. (4), we found that CHO and CN make a downward shift in both HOMO and LUMO levels, while CH_3 and OCH_3 make an upward shift in HOMO showing good agreement with DFT calculations [32]. In addition, we observed that functional groups whose valence orbitals are of π-symmetry seem to have more influence on the position of frontier orbitals in comparison to σ-symmetry. On the other hand, we found that the general shape of the zero-bias transmission spectra for all systems, shown as $T(E, V_b = 0)$ in Fig. (4), are similar, bringing the HOMO closer to E_F. So we focused on the qualitative effect of the functional groups on the HOMO of the contacted molecule. Two important

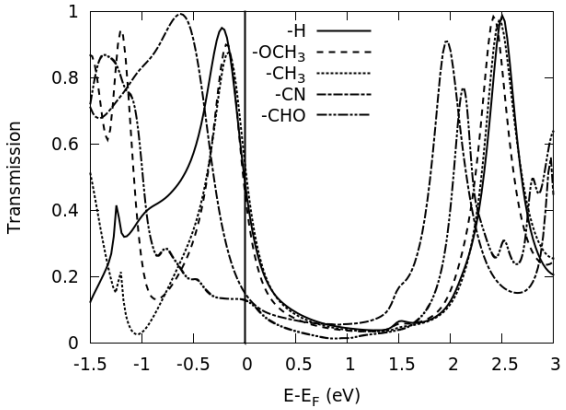

Fig. 4 – Zero bias transmission of adenine molecule with four different functional groups attached to the gold contacts *via* sulfur as a function of energy. Vertical line indicates the Au Fermi level.

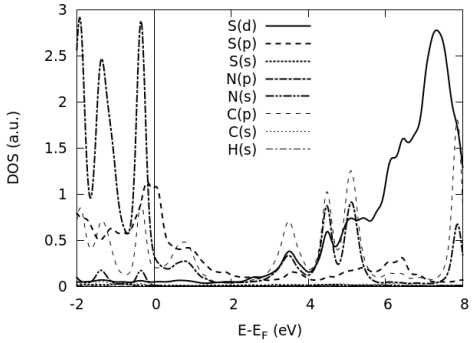

Fig. 5 – The projected density of states (PDOS) at each atom in the bare structure.

factors have to be considered to figure out the behavior of functional groups: the size of the lone pairs (or non-bonding pair) and the electronegativity of the element [31].

To understand the broadening of frontier molecular levels, we studied the projected density of states (PDOS) of the structures on each molecular orbital. It helps us to gain insight into the mechanism determining the band alignment and thus the conductance. As we see in Fig. (5), p-orbital of N, C and S atoms have main peaks in DOS plot near gold Fermi level. Then the HOMO is combined of some component of N atoms and $\mathrm{p}-\pi$ density on each of the two C atoms which are bonded to the N atom. Therefore, the behavior of the Nitrile group can be explained by the $\mathrm{N}(2\mathrm{p}\pi)$ lone pair in CN withdrawing the adenine π space, thereby lowering the energy of the HOMO. Similarly, when $\mathrm{OCH_3}$ substitute replace H atoms, the $\mathrm{O}(2\mathrm{p}\pi)$ lone pair delocalizes into the adenine π-space and the energy of the HOMO is raised. As

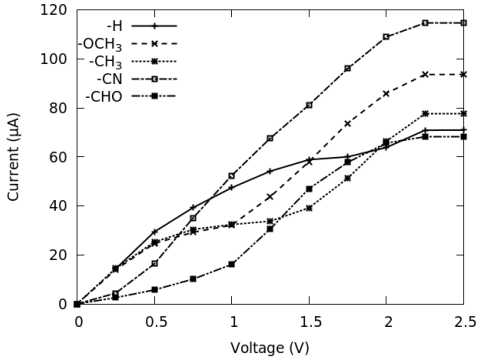

Fig. 6 – The current-voltage (I-V) curves for the bare and functionalized structures. The dashed lines are guides to the eyes.

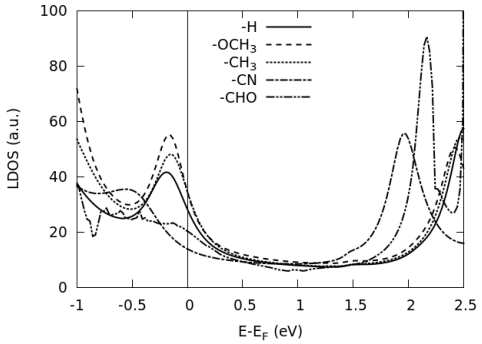

Fig. 7 – The local density of states (LDOS) of the adenine molecule device with different functional groups at zero-bias. Vertical line indicates the Au Fermi level.

for the methyl group, since carbon is slightly more electronegative than hydrogen, there will be a small dipole moment pulling electron density away from hydrogen toward carbon, resulting in HOMO being raised in energy. For the Aldehyde, the more electronegative O removes electron density from the σ-space of the adenine, thereby deshielding the π-space and therefore lowering the energy of the HOMO.

Figure 6 depicts the self-consistently calculated I-V curves in a bias range from 0 to 2.5V. Below 0.5V, the behavior of the I-V curves could be considered linear for all bare and functionalized adenine junctions but with a different trend for CN that seems to be exponential. To specify the origin of this behavior, we plotted the local density of states for all structures in Fig. (7). From this plot, we see that curves for all groups but CN have a main peak just below the Fermi level, with a non-zero amount of conductance at Fermi level, so they can be considered metallic. Furthermore for the voltages above 2V the functionalized adenine shows, in general,

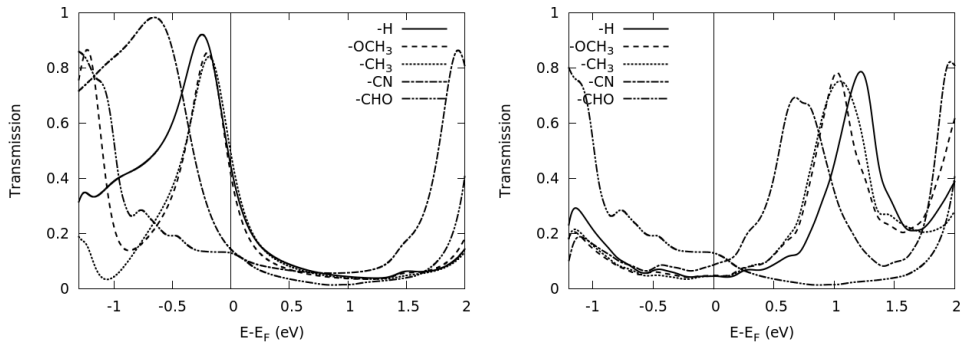

(a) (b)

Fig. 8 – Transmission of adenine molecule with three functional groups attached to the gold contacts *via* sulfur as a function of energy at (a) V = 0.5V and (b) V = 2V. Vertical lines indicate the Au Fermi level.

the higher current as compared to the bare one. The functionalization by CHO group, however, is found to be an interesting exception. We can order the current in this region as $I(\mathrm{CN}) > I(\mathrm{OCH_3}) > I(\mathrm{CH_3}) > I$(Bare adenine)$> I(\mathrm{CHO})$.

To explain the behavior of I-V curves, we plotted the transmission probability at two particular voltages. Figures 8a and 8b show the transmission probability for all functionalized groups in an electron energy range from -1.5 eV to 2.0 eV at bias voltages equal to 0.5 V and 2 V, respectively. The reason for selecting this two particular voltages is that the current shows completely different trends at these points. By increasing voltage, the HOMO and LUMO peaks undergo a downward shift in energy, so the transmission probability changes significantly. In addition, the current is proportional to the area under the transmission probability. At 0.5V (within voltage window of -0.5 to 0.5 eV), bare adenine has the biggest area under the transmission probability followed by $(\mathrm{OCH_3}) \simeq (\mathrm{CH_3})$, (CN), and (CHO) that is in good agreement with current order at this voltage. At 0.5V, the transmission is yet dominated by HOMO while at 2V, the LUMO peaks are responsible for transmission. Furthermore, at 2V, the CN has the largest area and as a result largest current followed by $\mathrm{OCH_3}$, $\mathrm{CH_3}$, H, and CHO functional groups.

4. CONCLUSION

Our studies on the electronic and transport properties of the functionalized adenine-based molecular junction showed that the conductance of the structures is strongly affected by the functionalization. We found that the functional groups with electron donating effects increase the molecule's conductance, whereas the electron

accepting groups decrease the conductance drastically. Similar results have been obtained previously, using the DFTB+NEGF method. The functional groups show different I-V characteristics so that all bare and functionalizaed adenine could be considered linear at lower voltages with an interesting exception of CN. At bias voltages higher than 2 V, the currents through the junctions are ordered as follows: $I(\mathrm{CN}) > I(\mathrm{OCH_3}) > I(\mathrm{CH_3}) > I(\text{Bare adenine}) > I(\mathrm{CHO})$ (in obvious notations).

Acknowledgements. We would like to thank Prof. Thomas Frauenheim, Bremen Center for Computational Material Science (BCCMS), for the permission to use DFTB+ on their cluster, as well as Dr. Vitalij Lutsker and Dr. Gabriele Penazzi for valuable discussions.

REFERENCES

1. H. Milani Moghaddam, M. Damchi Jelodar, *Indian J. Phys.* **87**, 99 (2013).
2. G. Peng, M. Strange, K. S. Thygesen, and M. Mavrikakis, *J. Phys. Chem. C* **113**(49) 20967-20973 (2009).
3. E. Leary, A. La Rosa, M. T. Gonzalez, G. Rubio-Bollinger, N. Agrait, and N. Martin, *Chem. Soc. Rev.* **44**, 920-942 (2015).
4. S. Yuan, S. Wang, Y. Wang, Z. Xu, Q. Ling, *Com. Mat. Sci.* **113**, 53-59 (2016).
5. L. Venkataraman, Y. S. Park, A. C. Whalley, C. Nuckolls, M. S. Hybertsen, and M. L. Steigerwald, *Nano Lett.* **7**(2) 502 (2007).
6. D. J. Mowbray, G. Jones, and K. S. Thygesen, *J. Chem. Phys.* **128**, 111103 (2008).
7. C. Preferencial Kala, P. Aruna Priya, and D. John Thiruvadigal, *Asian J. Chem.* **25**, S427-S429 (2013).
8. D. K. K. Randhawa, L. M. B. Inderpreet Kaur, M. L. Singh, *Int. J. Comput. Appl.* **17**(1) 8-12 (2011).
9. G. Schwabegger, M. Ullah, M. Irimia-Vladu, M. Baumgartner, Y. Kanbur, R. Ahmed, P. Stadler, S. Bauer, N. S. Sariciftci, H. Sitter, *Synthetic Met.* **161-66**(19-20) 2058-2062 (2011).
10. F. Pogacean, A. R. Biris, M. Coros, F. Watanabe, A. S. Biris, S. Clichici, A. Filip, S. Pruneanu, *Physica E.* **59**, 181-185 (2014).
11. I. Yanov, J. J. Palacios, and G. Hill, *J. Phys. Chem. A.* **112**(10) 2069-2073 (2008).
12. A. Pecchia, G. Penazzi, L. Salvucci, and A. Di Carlo, *New J. Phys.* **10**, 065022 (2008).
13. D. Porezag, T. Frauenheim, T. Kohler, G. Seifert, and R. Kaschner, *Phys. Rev. B.* **51**, 12947 (1995).
14. G. Seifert, D. Porezag, and T. Frauenheim, *Int. J. Quant. Chem.* **58**, 185 (1996).
15. M. Elstner, D. Porezag, G. Jungnickel, M. Haugk, T. Frauenheim, S. Suhai, and G. Seifert, *Phys. Rev. B.* **58**, 7260 (1998).
16. T. A. Niehaus, S. Suhai, F. Della Sala, P. Lugli, M. Elstner, G. Seifert, and T. Frauenheim, *Phys. Rev. B.* **63**, 085108 (2001).
17. T. A. Niehaus, *J. Mol. Struct.: THEOCHEM* **914**, 38 (2009).
18. H. A. Witek, S. Irle, G. Zheng, W. A. de Jong, and K. Morokuma, *J. Chem. Phys.* **125**, 214706 (2006).
19. G. Zheng, S. Irle, and K. Morokuma, *Chem. Phys. Lett.* **412**, 210-216 (2005).
20. S. Kaminski, M. Gaus, M. Elstner, *J. Phys. Chem. A.* **116**(48) 11927-37 (2012).
21. T. Frauenheim, G. Seifert, M. Elstner, T. Niehaus, C. Kohler, M. Amkreutz, M. Sternberg, Z. Hajnal, A. Di Carlo, and S. Suhai, *J. Phys. Condens. Matter.* **14**, 3015-3047 (2002).
22. M. Elstner and G. Seifert, *Phil. Trans. R. Soc. A.* **372**, 20120483 (2014).

23. W. Kohn and L. J. Sham, *Phys. Rev.* **140**, A1133 (1965).
24. J. C. Slater and G. F. Koster, *Phys. Rev.* **94**(6) 1498-1524 (1954).
25. A. Fihey, C. Hettich, J. Touzeau, F. Maurel, A. Perrier, C. Kohler, B. Aradi, and T. Frauenheim, *J. Comput. Chem.* **36**, 2075 (2015).
26. A. Di Carlo, M. Gheorghe, P. Lugli, M. Sternberg, G. Seifert, T. Frauenheim, *Physica B.* **314**, 86-90 (2002).
27. S. Datta. *Electronic Transport in Mesoscopic Systems.* Cambridge University Press, Cambridge (1995).
28. H. Hakkinen, *Nat. Chem.* **4**(6) 443-55 (2012).
29. M. Tachibana, K. Yoshizawa, A. Ogawa, H. Fujimoto, and R. Hoffmann, *J. Phys. Chem. B.* **106**, 12727-12736 (2002).
30. H. J. Monkhorst and J. D. Pack, *Phys. Rev. B.* **13**(12) 5188 (1976).
31. J. Clayden, N. Greeves, S. Warren, and P. Wothers. *Organic Chemistry.* Oxford University Press, Oxford (2001).
32. J. Taylor, M. Brandbyge, and K. Stokbro, *Phys. Rev. B.* **68**(12) 121101 (2003).
33. J. E. Han and V. H. Crespi, *Appl. Phys. Lett.* **79**(17), 2829 (2001).